From 3D Sensing to Printing: A Survey

LONGYU ZHANG, HAIWEI DONG, and ABDULMOTALEB EL SADDIK, University of Ottawa

Three-dimensional (3D) sensing and printing technologies have reshaped our world in recent years. In this article, a comprehensive overview of techniques related to the pipeline from 3D sensing to printing is provided. We compare the latest 3D sensors and 3D printers and introduce several sensing, postprocessing, and printing techniques available from both commercial deployments and published research. In addition, we demonstrate several devices, software, and experimental results of our related projects to further elaborate details of this process. A case study is conducted to further illustrate the possible tradeoffs during the process of this pipeline. Current progress, future research trends, and potential risks of 3D technologies are also discussed.

Categories and Subject Descriptors: A.1 [**Introductory and Survey**]; I.4.5 [**Image Processing and Computer Vision**]: Reconstruction; J.6 [**Computer-Aided Engineering**]

General Terms: Design, Algorithms

Additional Key Words and Phrases: 3D sensing technologies, 3D model reconstruction, 3D printers

ACM Reference Format:
Longyu Zhang, Haiwei Dong, and Abdulmotaleb El Saddik. 2015. From 3D sensing to printing: A survey. ACM Trans. Multimedia Comput. Commun. Appl. 12, 2, Article 27 (October 2015), 23 pages.
DOI: http://dx.doi.org/10.1145/2818710

1. INTRODUCTION

In the past few years, developments in computer, sensor, and printer capabilities have improved the areas related to three-dimensional (3D) technologies. Among them, techniques for precisely measuring and reconstructing 3D models have attracted increasing attention since the release of consumer-grade RGB-depth sensor Microsoft Kinect version 1 (v1) [Kinect 2010]. These technologies enable us to create or reconstruct 3D models of environments, objects, or even humans. Furthermore, 3D sensing technologies have become more practical with the development and public availability of 3D printers and 3D printing services, which make the transition from digital models to physical objects easier.

Although 3D digital models can be created using graphics and animation software, such as 3DMax, SketchUp, and Maya, this article focuses on 3D sensing from reality [Ikeuchi 2001] for 3D printing. The 3D sensing of an object usually involves acquiring data, building the point cloud, and converting the 3D model into a triangulated network (mesh) or textured surface [Remondino and El-Hakim 2006]. This field has been the subject of intensive and long-term research by the graphics, vision, and photogrammetric communities, and it is important and fundamental for applications such as cultural heritage digital archiving, virtual tourism, and virtual interaction systems. Large projects, such as the *Digital Michelangelo Project*, which created a 3D computer

Authors' addresses: L. Zhang, H. Dong, and A. El Saddik, Multimedia Communications Research Lab, University of Ottawa, 800 King Edward, K1N5N6 Ottawa, Canada; emails: {lzhan121, hdong, elsaddik}@uottawa.ca.

DOI: http://dx.doi.org/10.1145/2818710

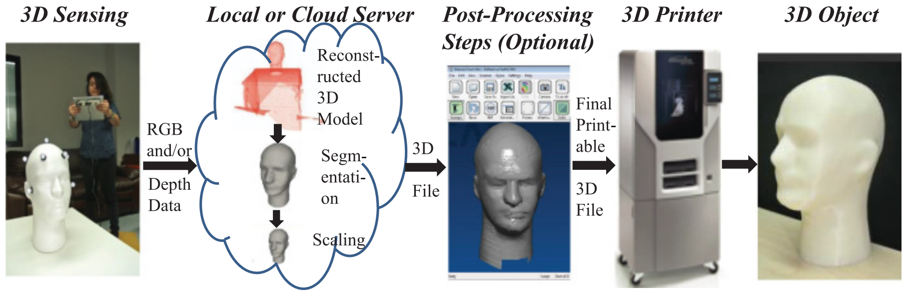

Fig. 1. System architecture: from 3D sensing to printing.

archive of many of Michelangelo's statues and architectural works, and the *Great Wall of China in 3D Project*, which aimed to recreate the whole 6,000km length of the Great Wall of China using high-resolution 3D models, are practical applications of 3D sensing technologies [Levoy et al. 2000]. Because different 3D sensing techniques have different requirements for light conditions (visible or invisible lights), result accuracy (for entertainment or medical use), and sensor configuration (a moving sensor or multiple sensors), users should choose an appropriate technique according to their specific requirements [Javidi et al. 2013; Zhu and Gao 2012].

After capturing 3D models from real objects or humans, we can use 3D printing technologies to physically reproduce them. 3D printing has existed for approximately 30 years but has only been available to the general public since the 2000s [Horvath 2014]. Currently, several companies, such as iMaterialise [i.materialise 2015] and Shapesways [2015], provide convenient online 3D printing services. Through these services, users can simply upload their 3D model files, choose the appropriate material, and get the printed 3D objects delivered to the designated address in a few weeks. In addition to these 3D printing service providers, there are also many high-end and hobby-level 3D printers available on the market. Unlike designing using 3D modeling software, reconstructing printable 3D models from reality may require the use of reconstruction algorithms and postprocessing steps [Liu and Niu 2012].

The aim of this survey is to provide a comprehensive overview of the techniques related to the pipeline from 3D sensing to printing, including 3D sensing and printing processes and devices, as well as techniques from both commercial deployments and published research.

This article is organized as follows. Section 1 discusses the general architecture of a 3D sensing-to-printing system. In Section 2, we explain the general 3D sensing process, commercially available 3D sensors, and the reconstruction process. Possible 3D model postprocessing steps and software are presented in Section 3. Section 4 addresses 3D printing research. Section 5 gives a practical case study. Finally, we summarize the article and present future research trends in Section 6.

2. GENERAL ARCHITECTURE OF A 3D SENSING-TO-PRINTING SYSTEM

In this section, we discuss the general architecture of a 3D sensing-to-printing system, as shown in Figure 1. First, the 3D sensors are used to scan the targeted object and continuously send RGB and/or depth data to a local or cloud server through a cable or WiFi network connection. The 3D data are then fed to appropriate 3D reconstruction algorithms. Using the completely reconstructed 3D model, segmentation and scaling algorithms are applied depending on the nature of the target and scans. The created printable 3D file (e.g., STL file) of the target, which occupies a water-tight mesh structure, is further modified with graphic tools if needed. The final printable 3D file is then sent to a 3D printer and transformed into a physical object made of the selected materials.

The advantages of considering the steps in the process as a whole are as follows: 3D model printing must be fully considered during the 3D sensing process, because the sensing configurations for other purposes, such as virtual environment reconstruction or augmented reality, are different; the postprocessing steps for 3D printing are also different from those for 3D animation development. Therefore, to successfully produce a 3D printed object, users need to carefully select the appropriate sensing process and sensors based on their scanned target and the desired level of detail, generate the desired printable water-tight (no holes) polygon meshes through postprocessing steps, and choose suitable 3D printing technology and materials.

3. 3D SENSING

With the rapid development of 3D technologies, such as 3D scene/model reconstructions, 3D holographic displays, and 3D movies, the demand for 3D contents is continually growing [Milani and Calvagno 2011]. Without a doubt, the launch of Microsoft Kinect v1 sensors further expanded this area because of their low consumer price, compact size, and ability to capture depth and image data at video rate. In this section, we focus on the general 3D sensing process, 3D sensors, the reconstruction process, and the limitations of current 3D sensing technology.

There are some existing papers surveying 3D sensors and sensing techniques. For example, Blais [2004] listed several commercialized 3D sensors that have persisted for years because of their robustness; Sansoni et al. [2009] reviewed some 3D sensing techniques and applications in industry, cultural heritage, medicine, and criminal investigation; Stoykova et al. [2007] surveyed several technologies used to capture and reconstruct 3D scenes for 3DTV displays, 3D extraction, or digital holography; and Opitz et al. [2012] compared the performance of 3D scanning technology with close-range photogrammetry in documenting excavation, ceramic vessels, rock art, and so forth. However, these papers mainly address the working principles of 3D sensor hardware or 3D reconstruction for virtual environment/augmented reality and do not give consideration to the whole pipeline of sensing and reconstructing printable 3D models for 3D printing, which is discussed comprehensively in our article. Additionally, several widely used 3D sensors and new versions of previous sensors, such as Kinect v1 and v2, have been released since the publication of these papers and have deeply influenced the current 3D sensor market. Moreover, with the improvements in 3D technologies, some sensing processes introduced in these papers have been further developed. For instance, stereo vision, which is discussed as a passive technique in Sansoni et al. [2009], has been fused with active time-of-flight sensors by Zhu et al. [2008] to achieve improved accuracy and robustness. Thus, in this section, we provide a more comprehensive overview of the general 3D sensing processes with consideration of 3D printing, compare several commercialized 3D sensors, and discuss the 3D reconstruction process.

3.1. General 3D Sensing Process

The general 3D sensing process mainly consists of capturing target information with sensors, merging the obtained information based on the sensing methods, and then reconstructing the 3D model. In this section, we divide the 3D sensing processes into three basic categories based on their different sensing configurations: adopting one moving sensor, adopting multiple sensors with different views, and adopting one sensor with a limited view, as shown in Figure 2. They have all achieved compelling results but differ in some attributes, such as speed, robustness, flexibility, computational cost, and completeness of the reconstruction [Barazzetti et al. 2010].

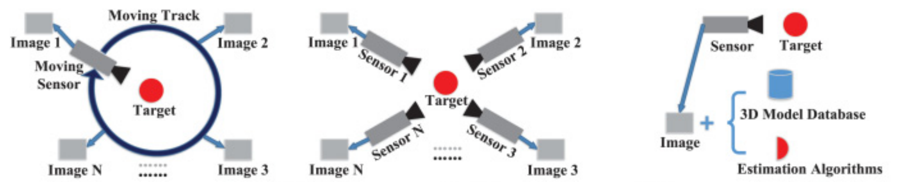

(a) One moving sensor. Moving one sensor around the target to obtain full views for 3D reconstruction.

(b) Multiple sensors with different views. Setting multiple sensors around the target, and then fusing their different views into one 3D representation.

(c) One sensor with limited view. Applying one sensor to obtain a limited view, and then reconstructing a rough 3D model with database or estimation algorithms

Fig. 2. Configurations of different 3D sensing processes.

3.1.1. Adopting One Moving Sensor. Although sensing the target with a fixed sensor from a single view is not sufficient to generate detailed 3D models, users can obtain the full set of 360-degree views of the physical scene or object by moving the sensor around the target or by rotating the object instead. Through fusing all of the sensed information, a single representation can then be reconstructed [Cui et al. 2010; Izadi et al. 2011]. Figure 2(a) shows the detailed configuration of this sensing process.

This sensing process has several advantages: (1) it enables the use of portable 3D sensors to scan large objects or scenes conveniently without complex configurations [Newcombe et al. 2011]; (2) the operating steps can be easily understood and conducted by common consumers, which facilitates commercialization and industrialization, such as the already marketed *ReconstructMe* system [Rooker et al. 2013]; (3) through carefully controlling the sensor's or turntable's rotating track, speed, and angles, if circumstances allow, accurate results can be obtained, such as the *Cyberware* scanner shown in Figure 3(a), as well as the project by Tong et al. [2012], which sets three Kinects v1 at different heights on the frame around the turntable to improve the depth resolution.

One major drawback of this sensing process is the requirement that the target should remain still for a long sensing duration, which is not suitable for situations such as sensing infants. Another drawback is the loop closure problem, because the sensing system sometimes fails to detect the completion of the scanning. As a result, the system cannot perfectly match the start scene with the ending scene to reconstruct the complete 3D model [Henry et al. 2014; Clemente et al. 2007]. Moreover, noises and inappropriate operation may degrade the reconstruction algorithms' performance. For example, individual pairwise errors would cause Iterative Closest Point (ICP) failure [Chatterjee et al. 2012].

3.1.2. Adopting Multiple Sensors with Different Views. Setting two or more fixed sensors around the target to capture the full views concurrently for 3D model reconstruction is another widely used 3D sensing process, as shown in Figure 2(b). It can be further divided into two categories: with sensor calibration (e.g., Photogrammetry) and without sensor calibration (e.g., Multiview Stereo, known as MVS). Photogrammetry usually consists of camera calibration and orientation, image point measurements, and 3D model generation [Sansoni et al. 2009]. Among these steps, sensor calibration is crucial to obtain accurate models, and reliable packages are commercially available to complete this phase, such as *Photomodeler* software by EosSystems [2015] and *Menci* by MenciSoftware [2015]. Conversely, MVS is more straightforward and cost-effective because its reconstruction is based on the identification of the common points within the image pairs. Generally, MVS algorithms can be classified into four categories based on the underlying object models: voxel based, deformable polygonal meshes based, multiple depth maps based, and patch based [Furukawa and Ponce 2010].

Reconstructing 3D models using multiple sensors with different views can achieve relatively high accuracy. For example, Rau and Yeh [2012] realized reconstruction results with the best accuracy of 0.26mm by carefully calibrating the digital single lens reflex cameras' exterior and interior orientation parameters using an optimized camera-location configuration (setting five sensors in two lines). The MVS methods introduced by Furukawa and Ponce [2010] also obtained considerably compelling results.

However, this 3D sensing process has certain limitations: (1) it always demands large amounts of computational resources, such as a Graphics Processing Unit (GPU) and powerful machines, to improve the performance [Zhang and Seah 2012]; (2) it is usually limited to well-defined scenes [Sansoni et al. 2009]; (3) adopting passive-image-based sensors may require calibration processes, experience problems with sparse textures and complex occlusions among different views, and be sensitive to light conditions; and (4) utilizing multiple active sensors simultaneously could cause a certain level of interference and accuracy degradation [Wang et al. 2012; Kang and Ho 2010].

3.1.3. Adopting One Sensor with Limited View. Despite the rapid development of 3D sensing technologies, there are still situations in which users cannot move the sensor or use multiple sensors to obtain the full views of the target. If 3D reconstruction is still required in this case, appropriate estimations or 3D model database matching may need to be applied to reconstruct rough and approximate 3D models rather than detailed ones, as shown in Figure 2(c). Some techniques, such as shape from focusing, shape from shadows, shape from shading, and shape from photometry, are indirect, simple, and low-cost ways to solve this problem [Ciaccio et al. 2013; Adm and Said 2012]. Utilizing a collected or learned 3D database to match the acquired 2D images is also widely adopted in reconstructing objects or scenes. Patel and Zaveri [2012] reconstructed 3D human head models by extracting features from the 2D detected face and then combined the features with the matched 3D head model from the database.

Although this 3D sensing process is capable of generating 3D models from limited views conveniently and inexpensively, the obtained results are usually subject to the estimation algorithms or matched database and are not suitable for precise reconstructions. Therefore, this process is used as a compromise when the other two sensing processes cannot be implemented.

3.2. 3D Sensing Devices

As mentioned previously, the release of consumer-grade Microsoft Kinect v1 sensors attracted large amounts of attention to 3D sensing research. In fact, long before Kinect v1 was available, several types of sensors adopting various technologies were developed and/or marketed to satisfy these demands. In the following section, we introduce and compare several commonly used sensing devices and their working principles.

Sensors are usually used to measure the shape and appearance of physical objects or the environment and then generate dense point clouds or polygon meshes to reconstruct the target. Traditional passive-image-based cameras, which are only capable of capturing 2D images without depth information, can be used as 3D sensors with careful calibration, feature matching among images, and/or depth estimation algorithms [Rau and Yeh 2012; Patel and Zaveri 2012; Zhang et al. 2014]. Additionally, active 3D sensing devices have a variety of working principles. In this article, we mainly focus on active 3D sensing devices. Figure 3 shows several commercially available active 3D sensing devices that adopt different working principles, including triangulation-based laser, structured-light, time-of-flight, and X-ray computed tomography.

3.2.1. Triangulation-Based Laser Sensing Devices. Triangulation-based laser sensors usually shine a laser on the subject and employ a camera to measure the location of the laser dot, and then, based on the distance of the object the laser strikes, the laser dot

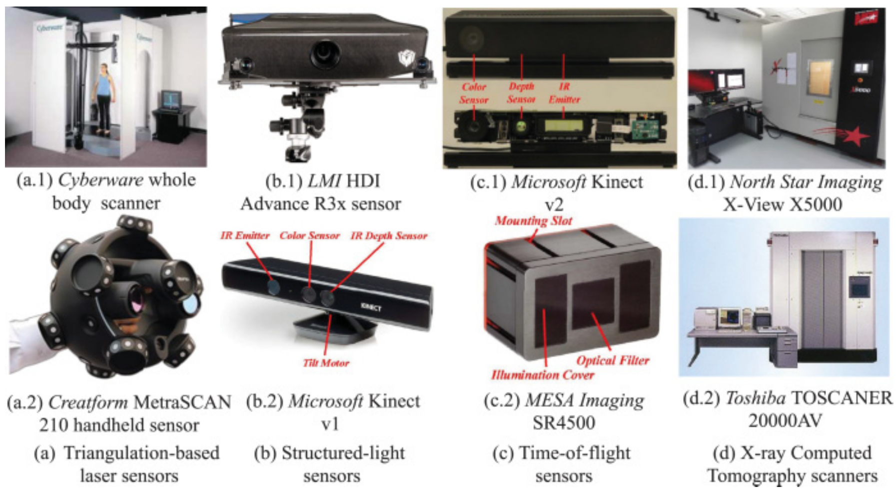

Fig. 3. Several commercially available 3D sensing devices [Cyberware 2015; Creatform 2015; Technologies 2015; Microsoft 2015; MESA-Imaging 2015; North-Star-Imaging 2015; Toshiba 2015].

appears at different places in the camera's field of view. This method is called triangulation because the laser dot, the camera, and the laser emitter form a triangle [Žbontar et al. 2013]. These types of sensors are usually able to acquire high-quality data to build precise 3D object models but are expensive compared with other sensors and require expert knowledge to operate. Examples include the Cyberware Whole Body Color 3D Scanner, NextEngine desktop 3D scanner, and Creaform's handheld HandyScan scanner [Cyberware 2015]. Moreover, users are always required to stand still during the capturing process, which is difficult in some situations, such as sensing 3D models for infants [Allen et al. 2003].

3.2.2. Structured-Light Sensing Devices. Structured-light devices usually project patterns consisting of many stripes at once or of arbitrary fringes, which allows the acquisition of many samples simultaneously. Working as 3D sensors, they offer several advantages at affordable prices and have attracted large amounts of attention from researchers worldwide [Tong et al. 2012; Zhou et al. 2013; Sturm et al. 2013]. Structured-light devices have the following capabilities: (1) capturing depth images at video rate in low light levels, (2) operating safely for both the user and the scanned object with easy operation similar to that of video cameras, (3) solving silhouette ambiguities in pose, (4) simplifying the background subtraction process, and (5) easily synthesizing realistic depth images of people [Liu et al. 2010a; Salvi et al. 2010; Liu et al. 2010b; Shotton et al. 2011].

Structured-light devices have not yet begun to dominate the 3D scanning market because they were not originally designed as high-quality 3D sensors and were instead developed for object detection and as part of natural user interfaces [Cui et al. 2013]. As a result, they usually have low X/Y resolution and high noise levels, which always affect their accuracy. For example, the first consumer-grade structured-light Kinect v1 had rather low resolution (640×480 pixels for RGB images and 640×480 pixels for depth images), which usually results in just-acceptable accuracy in reconstructing 3D models. However, researchers are still attempting to further improve their performance. Wijenayake et al. [2012] proposed an error-correcting technique to improve the 3D scanning results of the structured-light method, and Smisek et al. [2013] suggested an algorithm that allowed Kinect v1 to outperform SwissRanger ToF SR4000 in accuracy when measuring planar targets.

3.2.3. Time-of-Flight Sensing Devices. Time-of-Flight (ToF) sensors are different from structured-light sensors in their working principles. They use active sensors to measure the distance of a surface by calculating the round-trip time of the emitted infrared light, and commercially available ToF cameras usually employ homodyning methods and operate in continuous mode [Kolb et al. 2009]. ToF sensors do not interfere with the scene in the visual spectrum because they use infrared light. They are usually more expensive than structured-light cameras but cheaper than triangulation laser sensors.

ToF sensors emerged around the year 2000 as the semiconductor process became fast enough to handle such devices and were first introduced by Lange and Seitz [2001], who successfully realized an all-solid-state 3D ToF range sensor. Later, Gokturk et al. [2004] introduced ToF sensors to the graphics and vision community by integrating a complete ToF sensor with a complementary metal oxide semiconductor chip to develop highly cost-effective 3D sensors. ToF sensors have capabilities similar to those of structured-light sensors, such as the capturing of depth images at video rate in low light levels, color and texture invariance, and the ability to resolve silhouette ambiguities in pose. However, ToF sensors also have drawbacks: (1) they suffer from signal-dependent shot noise, because the process of measuring instantaneous light power with semiconductor substrates involves the conversion from photon energy to electron displacement [Kirmani et al. 2013]; (2) they exhibit random noise and a notable systematic measurement bias [Anderson et al. 2005]; (3) their images are sometimes compromised by scattering and motion blur problems [Hansard et al. 2012]; and (4) they usually capture depth images at low resolution [Cui et al. 2013]. Among ToF companies, MESA Imaging produced the Swiss Ranger SR4k family [MESA-Imaging 2015], PMD developed the PhotonlCs series [Möller et al. 2005], Canesta developed CanestaVision, and Microsoft created Kinect v2 [Yang et al. 2015].

3.2.4. X-Ray Computed Tomography Sensing Devices. Although conventional computed tomography (CT) is a medical imaging technology used to generate a 3D image of the inside of an object, industrial X-ray CT can reconstruct a 3D model of both the internal and external structures of the scanned object from a number of 2D images obtained using X-ray radiation in many positions around an axis of rotation [Kruth et al. 2011]. As a nondestructive sensing technology, X-ray CT is able to measure both the outer and inner geometries of a solid object without the need to cut through or destroy it. X-ray CT can also have rather high resolution or density; for example, X-View X5000, as shown in Figure 3(d), has a best resolution of 500*nm*. Another benefit is that it can scan various surfaces, shapes, colors, and materials with certain densities and penetrable thicknesses [De Chiffre et al. 2014].

X-ray CT has the following limitations: (1) it can only sense objects within its maximum penetrable thickness and otherwise may result in low-quality X-ray images because the object absorbs too much energy; (2) X-ray is inherently noisy, as are the detector and its amplification, which limits the X-ray CT's performance; (3) most industrial X-ray CTs cannot work with live body scan; and (4) scanning a multimaterial object may fail if the sensing device cannot detect the change in the material properties [Ketcham and Carlson 2001; De Chiffre et al. 2014].

3.2.5. Comparison of Sensing Devices. Table I lists the details of the different types of 3D sensors in Figure 3. The technical data in the table were obtained from published papers [Khoshelham and Elberink 2012; Blais 2004; Tang et al. 2014], from official product data sheets, or by contacting the companies directly. The Cyberware 3D whole-body scanner bundle can scan the entire human body in approximately 17 seconds;

Table I. Comparison of 3D Sensing Devices

Type	Triangulation-Based Laser		Structured Light	Time of Flight			Computed Tomography	
Scanner	Cyberware Whole Body	Metra-SCAN 210	HDI Advance R3x	Kinect Version1	Kinect Version2	Swiss-Ranger SR4500	XView X5000	TOSC-ANER 20000AV
Price (2015)	\$240,000	\$70,000	\$25,000	\$100	\$200	\$5,000	N/A	N/A
Dimensions (cm×cm×cm)	261×290 ×235	28.2×25 ×28.2	25.4×15 ×10	28×6.35 ×7.62	24.9×6.6 ×6.7	11.9×7.5 ×6.9	200×274 ×232	200×270 ×255
Depth Range (m)	0–2	0.152–3	0.3–1	0.4–3	0.5–4.5	0.8–9	2.4	0.3–0.6
Depth Accuracy (cm)	0.03	0.0085	0.0045	3	2	2	N/A	N/A
Depth RES(mm)	0.5	0.05	0.075	@2m distance 10	5	5	0.0005	0.1
Depth Image Max RES	60,000 points	36,000 points	2.6M pixels	640×480 pixels	512×424 pixels	176×144 pixels	N/A	N/A
RGB Image Max RES	N/A	N/A	N/A	1280 ×960	1920 ×1080	N/A	N/A	N/A
Max FPS	N/A	N/A	1.14	30	30	30	N/A	N/A

Note: RES represents resolution, and FPS represents frames per second.

store the array of digitized points in terms of X, Y, and Z coordinates for shape; and use 24-bit RGB values for color. The scanning speed is 60,000 points per second, and the density is 70 points per square centimeter. Kinect for Windows comes in two versions (v1 and v2). V1 dramatically influenced the depth sensing market, while v2 offers higher-resolution RGB images and a less noisy depth stream compared with v1. Additionally, Kinect v2 adopts ToF technology instead of structured light, which was used in v1. SwissRanger SR4500 is an industrial-grade ToF camera developed by Mesa Imaging. It has relatively high accuracy and stability. Multicamera operation (more than three cameras) has been supported in its software to suit broader applications. Moreover, X-View X5000 has a relatively high resolution of 500*nm*, as mentioned previously.

3.3. Reconstructing Process

In this part, we address the process of reconstructing 3D models with sensed information from a moving sensor or multiple sensors. To fuse these captured data into a single 3D model properly, registration plays an important role. This process estimates the rigid motion (translations and rotations) of a set of points with respect to another set of points, which can be image pixels or 3D points.

Registration methods can be classified as extrinsic based, intrinsic based, and calibration based [Markelj et al. 2012]. To track and match corresponding points, extrinsic-based methods use external artificial markers; intrinsic-based methods use the subjects' own features, intensity, or gradient; and calibration-based methods utilize the precalibration process to realize this goal. Among these methods, intrinsic-based registration methods have the fewest restrictions in terms of users or locations. Coarse registration, fine registration, or both can be used to estimate the rigid motion. Coarse registrations are usually random-sample-consensus-based methods that use sparse feature matching [Feldmar and Ayache 1996]; fine registration relies on minimizing point-to-point, point-to-plane, or plane-to-plane correspondences, such as the Iterative Closest Point (ICP) method, which iteratively revises the transformation of the source cloud to minimize its distance to the target cloud for achieving the best match [Zhang 1994; Chen and Medioni 1992]. Izadi et al. [2011] introduced a real-time 3D reconstruction algorithm, KinectFusion, which tracks the global pose of a moving Kinect with an

Table II. Comparison of 3D File Formats

	Binary	ASCII	Color	Material	Texture
STL	Y	Y	N	N	N
OBJ	N	Y	Y	Y	Y
VRML	N	Y	Y	Y	Y
PLY	Y	Y	Y	Y	Y
X3D	Y	Y	Y	Y	Y

ICP algorithm using a GPU and then fuses the dense depth data streamed from Kinect into a 3D volumetric surface representation. Based on KinectFusion, Sturm et al. [2013] developed *CopyMe3D* to scan and print persons in 3D based on this algorithm, while Rooker et al. [2013] developed *ReconstructMe*. Since ICP would fail to work when scans are noisy, Chatterjee et al. [2012] proposed an adaptive bilateral filter to smooth the depth image noise captured by structured-light sensors to overcome the failure caused by individual pairwise ICP errors and thus obtain accurate and consistent alignment.

In fact, many commercialized 3D sensors come with bundled software packages for automatic and convenient 3D reconstruction and visualization. Take the sensing devices in Figure 3 as examples: X-View X5000 is bundled with X-View software, the Cyberware Whole Body 3D scanner can be controlled via Cyberware software, SwissRanger SR4500 works with SR_3D_View, and Kinect v1 and v2 are both compatible with KinectFusion.

3.4. Limitations of 3D Sensing

Using various 3D sensing processes and devices, we can acquire 3D models indoors or outdoors, during the day or at night, with small or large sizes, and from inanimate materials or live human bodies. However, 3D sensing technologies still have certain limitations [Levoy et al. 2000]: (1) working with optically uncooperative materials, such as fuzzy hair, shiny parts, and translucent and transparent objects (e.g., lenses and glasses), can degrade the accuracy of the results; (2) scanning the inside structures of delicate objects, which cannot be entirely scanned from the outside, may cause collisions and thus damage the objects; (3) acquiring data from large objects may require downsampling the result to reduce the complexity; and (4) certain laser wavelengths cannot be used for live animals or humans. Thus, users should choose the appropriate 3D sensing process and sensor type to fulfill their specific purposes.

4. 3D MODEL POSTPROCESSING

Compared with models that were directly designed using modeling software packages, the data created using 3D sensors may require further optimization involving filling surface holes, changing to a particular file format, or improving the models to generate the desired printable water-tight (no holes) polygon meshes before 3D printing. In this section, we first discuss several 3D file formats that are used for both 3D sensing and 3D printing, and then we introduce and compare related 3D graphics tools.

4.1. 3D File Formats

Currently, many file formats exist for both 3D sensing and 3D printing, including STereoLithography (STL), Polygon (PLY), OBJ, Virtual Reality Modeling Language (VRML), and X3D [Ellerin 2004; Marcoux and Bonin 2012]. Table II presents several commonly used file formats and their features.

The most commonly used format is probably the STereoLithography (STL) file format [Iancu et al. 2010]. STL was developed by the *Alber Consulting Group* in 1987 to print 3D CAD models with 3D Systems stereolithography machines. It represents the outside surface of an object with a large number of tiny triangular meshes and provides a relatively straightforward way to describe the geometry of a 3D object in a manner that can be used by 3D printers. Besides, STL files can be created in both binary and ASCII format. The drawback of STL format is that it does not contain color, texture, and material information.

The Polygon File Format (PLY) was primarily designed to store 3D data from 3D sensors. It describes each object simply using a list of nominally flat polygons [Kaveh et al. 2013]. Compared with the STL format, PLY can contain several properties, such as color, texture coordinates, transparency, data confidence values, and surface normals.

Virtual Reality Modeling Language (VRML) is a standard file format used to represent 3D interactive vector graphics [Pan et al. 2013]. It can be utilized to specify a 3D polygon's vertices and edges, as well as the surface color, shininess, UV-mapped textures (U and V denote the axes of the 2D texture), and transparency. Because VRML was designed specifically for the World Wide Web, a web browser might fetch a webpage or a new VRML file from the Internet when users click on the specific graphical component.

X3D is a standard eXtensible-Markup-Language (XML)-based file format and a successor to VRML [Brutzman and Daly 2010]. It is based on both XML syntax and Open Inventor-like syntax, and it offers enhanced Application Programming Interfaces.

OBJ, developed by *Wavefront Technologies*, is featured with its advanced visualizer animation package [Wang and Yao 2011]. It has been adopted by many 3D graphics application vendors and has become a universally accepted format. OBJ consists of a number of lines containing keywords and various values, as this file format does not require a header.

Digital Asset Exchange (DAE), SKP, 3DS, and many other 3D file formats are also used by certain 3D software packages. Thus, users need to choose the appropriate 3D file format based on their utilized sensing software package, postprocessing tools, and 3D printer to ensure that the selected file format will work with all of the aforementioned tools.

4.2. 3D Graphics Tools

Both open-source and proprietary 3D graphics tools are commercially available to acquire, convert, and/or modify digital 3D object files. Free software packages such as Blender, ADMesh, and MeshLab are all distributed under the GNU General Public License (GPL) terms [Hacıoğlu 2014], which guarantee the freedom to share and change all versions of a program. Proprietary software packages, such as Maya, 3ds Max, SketchUp, and AC3D, are also available.

3D graphic tools usually differ from each other in areas of copyright, compatible operating systems, importable file formats, and some postprocessing functions, as listed in Table III. These tools include the following: (1) Blender offers full features and supports the entire 3D pipeline as an open-source suite, which has increased its popularity in this domain [Slavkovsky 2012]. (2) MeshLab has special versions for mobile operating systems, such as Android and iOS, which offers more convenience for mobile application development. (3) AdMesh mainly works with Linux systems and only reads the STL file format, which does not have the color painting function. AdMesh features the ability to check STL files for flaws (e.g., unconnected facets and bad normals), repair facets by connecting nearby facets with a given tolerance, and fill holes in the mesh by adding facets. (4) Art of Illusion (AoI) is programmed with Java, which can be run on any computer that supports Java 5 or later [Fish 2011]. (5) Maya and 3ds Max are both comprehensive 3D graphics tools with multiple functions, but the former does not support 3DS and PLY file formats, while the latter only works with Windows operating systems. Finally, (6) SketchUp is one of the easiest tools to start with because it offers

Table III. Comparison of 3D Graphic Tools

<table>
<tr><th colspan="2"></th><th>Blender</th><th>ADMesh</th><th>MeshLab</th><th>AoI</th><th>Maya</th><th>3ds Max</th><th>SketchUp</th><th>AC3D</th></tr>
<tr><td colspan="2">Proprietary</td><td>N</td><td>N</td><td>N</td><td>N</td><td>Y</td><td>Y</td><td>Y</td><td>Y</td></tr>
<tr><td rowspan="5">Compatible OS</td><td>Windows</td><td>Y</td><td>N</td><td>Y</td><td>Y</td><td>Y</td><td>Y</td><td>Y</td><td>Y</td></tr>
<tr><td>Mac</td><td>Y</td><td>N</td><td>Y</td><td>Y</td><td>Y</td><td>N</td><td>Y</td><td>Y</td></tr>
<tr><td>Linux</td><td>Y</td><td>Y</td><td>Y</td><td>Y</td><td>Y</td><td>N</td><td>N</td><td>Y</td></tr>
<tr><td>Android</td><td>N</td><td>N</td><td>Y</td><td>N</td><td>N</td><td>N</td><td>N</td><td>N</td></tr>
<tr><td>iOS</td><td>N</td><td>N</td><td>Y</td><td>N</td><td>N</td><td>N</td><td>N</td><td>N</td></tr>
<tr><td rowspan="8">Functions</td><td>Modeling</td><td>Y</td><td>Y</td><td>Y</td><td>Y</td><td>Y</td><td>Y</td><td>Y</td><td>Y</td></tr>
<tr><td>Smoothing</td><td>Y</td><td>Y</td><td>Y</td><td>Y</td><td>Y</td><td>Y</td><td>Y</td><td>Y</td></tr>
<tr><td>Resizing</td><td>Y</td><td>Y</td><td>Y</td><td>Y</td><td>Y</td><td>Y</td><td>Y</td><td>Y</td></tr>
<tr><td>Hole Filling</td><td>Y</td><td>Y</td><td>Y</td><td>N</td><td>Y</td><td>Y</td><td>Y</td><td>Y</td></tr>
<tr><td>Color Painting</td><td>Y</td><td>N</td><td>Y</td><td>Y</td><td>Y</td><td>Y</td><td>Y</td><td>Y</td></tr>
<tr><td>Distance Measure</td><td>Y</td><td>Y</td><td>Y</td><td>Y</td><td>Y</td><td>Y</td><td>Y</td><td>Y</td></tr>
<tr><td>Point Cloud Input</td><td>Y</td><td>Y</td><td>Y</td><td>Y</td><td>N</td><td>Y</td><td>Y</td><td>Y</td></tr>
<tr><td>Cleaning Filter</td><td>Y</td><td>Y</td><td>Y</td><td>Y</td><td>Y</td><td>Y</td><td>Y</td><td>Y</td></tr>
<tr><td rowspan="6">Import File Formats</td><td>STL</td><td>Y</td><td>Y</td><td>Y</td><td>N</td><td>Y</td><td>Y</td><td>Y</td><td>Y</td></tr>
<tr><td>3DS</td><td>Y</td><td>N</td><td>Y</td><td>N</td><td>N</td><td>Y</td><td>Y</td><td>Y</td></tr>
<tr><td>OBJ</td><td>Y</td><td>N</td><td>Y</td><td>Y</td><td>Y</td><td>Y</td><td>Y</td><td>Y</td></tr>
<tr><td>VRML</td><td>Y</td><td>N</td><td>Y</td><td>N</td><td>Y</td><td>Y</td><td>Y</td><td>Y</td></tr>
<tr><td>PLY</td><td>Y</td><td>N</td><td>Y</td><td>N</td><td>N</td><td>N</td><td>Y</td><td>N</td></tr>
<tr><td>DXF</td><td>Y</td><td>N</td><td>N</td><td>N</td><td>Y</td><td>Y</td><td>Y</td><td>Y</td></tr>
</table>

an intuitive way to design 3D models, although designing and manipulating accurate models is difficult.

The state of the art of 3D model postprocessing techniques is still developing. For example, Xia and Chen [2014] proposed a new hole repairing algorithm that used an advancing front mesh technique to cover the hole with newly created triangles, and Pellerin et al. [2014] proposed a method to automatically remesh a 3D model surface using global Centroidal Voronoi optimization. With these developments, the postprocessing steps between 3D sensing and 3D printing would become more precise and convenient and easier.

5. 3D PRINTING

After obtaining the final printable 3D object digital files, we can send them to a 3D printer to produce the physical objects. The first 3D printer was built by Charles Hull, who invented Stereolithography technology to create tangible 3D objects from digital data. Later, the Massachusetts Institute of Technology (MIT) developed and patented inkjet-based 3D printing technology. Although the technology entered the marketplace then, it was not a viable alternative to traditional manufacturing due to the limited material usage, inconsistent accuracy, high price, and long production time. However, 3D printing technologies have shown explosive growth since the 2000s because of their availability to the public at affordable prices and open-source technology. The RepRap (short for Replicating Rapid prototype) project, an open-source project built in 2005 for the creation of inexpensive 3D printers, has made all its designs and software packages publicly available and improved under the GPL terms after some of the initial 3D-printing-related patents expired [Sells et al. 2009]. Its goals are to make the RepRap machine self-replicate and let 3D printing technology become available to everyone. In 2008, RepRap released Darwin, its first self-replicating printer able to print the majority of its own components. Later, MakerBot printers [Pettis et al. 2012] were created based on the RepRap design.

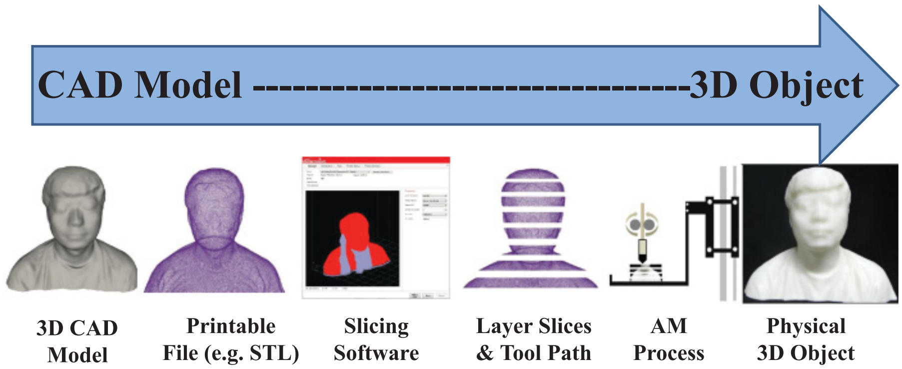

Fig. 4. General 3D printing process.

Both high-end and low-end 3D printers are available on the market. High-end printers involve expensive high-powered energy sources and complex techniques, and are able to print complex objects and even functional human tissue/organs. Conversely, low-end printers focus on reducing the complexity and cost of a well-established Additive Manufacturing process to bring the technology to the majority of the world [Campbell et al. 2011]. In the current market, many 3D printers are sold for under $1,000 with easy setup phases and improved quality, but commercial-grade printers remain expensive. Formlabs, MakerBot, Mcor Technologies, Organovo, and Sculpteo were highlighted as “the five cool vendors for 3D printing” by Gartner, an information technology research and advisory company [Gartner 2015].

5.1. General 3D Printing Process

3D printing is also called Additive Manufacturing (AM) because the final product is constructed from accumulations of raw material, which is opposite to the traditional Subtractive Manufacturing that cuts or molds raw materials into the desired shapes. Figure 4 shows the general 3D printing process. 3D models are fed into 3D software to create printable 3D files, which are divided into thin 2D slices using slicing software packages. The generated slices are sent to the 3D printer to be built up layer by layer until the whole object is obtained.

Because 3D printing hardware is now able to print continuous mixtures of multiple materials with increasing resolution and larger object size, challenges related to high computational demands, such as dealing with trillions of voxels and petabytes of data, simplifying 3D models efficiently, and spatially describing various combinations of materials, have arisen. Therefore, many researchers are proposing solutions to optimize multimaterial 3D printing, such as OpenFab [Vidimče et al. 2013] and Spec2Fab [Chen et al. 2013].

5.2. 3D Printing Technologies

3D printing technologies are mainly based on ink-jet principles and can print using a variety of materials, including plastic, resin, titanium, polymers, ceramics, gold, and silver [Horvath 2014; Marcoux and Bonin 2012]. We illustrate the printing principle of Fuse Deposition Modeling (FDM) in Figure 5 to show an example of 3D printing technologies. FDM prints the 3D object layer by layer from the bottom to the top through heating and extruding thermoplastic or wax filament [Campbell et al. 2011].

Currently, there are many types of 3D printing technologies to satisfy the market requirements. In the following section, we introduce several commonly used methods, including Stereolithography (SLA), Fuse Deposition Modeling (FDM), Direct Metal

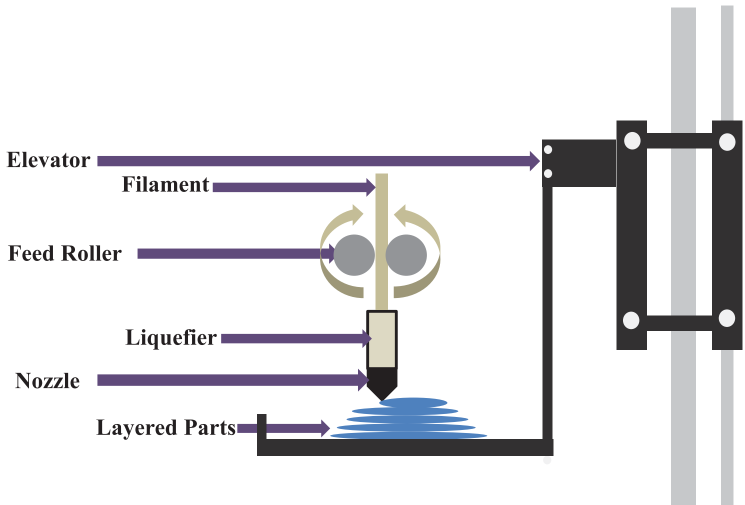

Fig. 5. Fuse Deposition Modeling (FDM) 3D printing principle.

Laser Sintering (DMLS), Selective Laser Sintering (SLS), Selective Laser Melting (SLM), and Electron Beam Melting (EBM).

Stereolithography: SLA uses an ultraviolet (UV) laser to draw the design on the surface of the liquid material and simultaneously hardens/solidifies the contacted material to build each layer. After finishing printing, the built part can be carefully removed from the liquid and taken from the platform. The first SLA machine was produced by the *3D Systems* company, founded by Charles Hull, the inventor of SLA technology [Horvath 2014]. SLA printers always have high precision and accuracy but require support structures and some postprocessing steps, compared with SLS printers.

Fuse Deposition Modeling [Ahn et al. 2002]: As shown in Figure 5, FDM uses a high-temperature nozzle to heat the thermoplastic or wax material to a semiliquid state and then deposit it along the designed path to print the 3D object layer by layer. FDM was developed in the late 1980s and commercialized in 1990, and it has become the standard hobby printer method. FDM usually requires users to adjust the printing process by adding sophisticated controls (e.g., supporting structures). Through the placement of soluble release material in the gaps between the movable parts, Lipson et al. [2005] from Cornell University reproduced several Reuleaux-Voigt kinematic models with FDM technology.

Polyjet [Vaupotič et al. 2006]: Polyjet is one of the currently leading rapid prototyping technologies that was developed by an Israeli company Object Geometries. It uses a carriage, which carries four or more inkjet heads and UV lamps, to deposit tiny droplets of photopolymers and thus print the 3D object. Compared with FDM, Polyjet requires more support material to restrain the tiny liquid droplets. Advanced Polyjet printers, such as Stratasys's Object Connex series and Object 1000, can print with multiple materials simultaneously, which allows users to incorporate various properties and colors into the 3D printed models.

Direct Metal Laser Sintering [Manfredi et al. 2013]: DMLS uses a laser as the power source to sinter the powdered material (especially metal) by aiming the laser automatically at points in space according to the imported 3D digital file, and then it binds the material together to create a solid structure. It is similar to SLS but differs in its technical details. DMLS can be used to produce metal parts for several applications, such as prototypes, series products, and production tools. One disadvantage of DMLS technology is that it is time-consuming to remove the metallic support structure and postprocess the generated part.

Selective Laser Sintering [Beard et al. 2011]: SLS machines use a high-power laser to fuse small particles of plastic, metal, ceramic, or glass powders according to the imported 3D model and then bind the material together to create a solid 3D product. The feature of this technology is that it processes the material during the sintering phase, in which the material never reaches a liquid phase (i.e., melting). Compared with SLA and FDM, SLS does not require supporting structures because the part being processed is surrounded by unsintered powder at all times. As a result, SLS is able to construct more elaborate geometries.

Selective Laser Melting [Mumtaz and Hopkinson 2010]: SLM is very similar to SLS in terms of its procedures. It fuses fine metallic powders together with a high-powered laser beam to build the 3D metal parts. During the process, materials are able to reach a liquid phase. However, compared with SLS, this technology may cause surface roughness because its high heat input often increases material vaporization and spatter generation.

Electron Beam Melting [Dehoff et al. 2013]: EBM has a similar process to SLM, but it uses an electron beam as its energy source instead of a laser. By using a vacuum, it eliminates the potential for contamination/oxidation at elevated temperatures. Because fabrication errors, such as contamination of the material, are important for accuracy, EBM is considered more advanced than SLS and SLM technologies. The disadvantage of this technology is that the system produces X-rays during operation.

5.2.1. Printer Comparison. With seemingly endless types of new 3D printers flooding the market, it is not easy to decide which printer is the most suitable. Generally, most inexpensive or hobby-level 3D printers may offer users the enjoyable Do-It-Yourself experience at affordable prices, but they are not able to create smooth and accurate 3D printed models that can act as low-cost working prototypes. Conversely, high-end printers can print objects with greater detail and higher quality.

In Table IV, we list the details of several commercially available printers. These printers adopt various 3D printing technologies (e.g., SLA, FDM, Polyjet) and can print objects with various materials and sizes. These machines may be shipped in several parts or fully assembled from 3D printer companies, such as *Stratasys*, *FormLab*, *Makerbot*, and *3D Systems*. Therefore, when making choices, consumers may need to consider the specifications and the requirements of their intended products/prototypes.

Users need to be careful with some parameters to obtain a good-quality printed object when working with 3D printers: new printers may require calibration to prevent lopsidedness; the axis of a circular part should be kept vertical; the nozzle and platform need to be heated according to the system's instructions before printing; large models require approximately 4 hours or more to print; the correct powder needs to be selected to create the desired thickness; and the appropriate ink should be chosen by considering the viscosity, particle size, and surface tension, which may affect the droplets deposited by the print head [Utela et al. 2008].

5.2.2. Printing Services. For companies or individuals who do not own 3D printers, web-based 3D printing services can be an alternative choice. Users can simply upload their 3D object files to the website, choose the preferred materials, pay the price calculated by the provider, and receive the delivered 3D-printed objects in a few days. Although this process requires much more time than using local 3D printers, it satisfies a large part of the market and has more options for materials. Table V lists some materials available from 3D printing services and their properties, such as minimum wall thickness, minimum detail, accuracy, clearance, and multicolor. Among the 3D printing

Table IV. Comparison of 3D Printers

	Company	Printable area (cm^3)	Assembled	Dimensions (cm^3)	Min Layer Thicknes (microns)	Nozzle (mm)	Filament (mm)	Min layer RES (microns)	Weight (kg)	Printing speed (mm/s)	Price (2014) (10^3\$)	Printable material	Technology type	Multicolor printing
Form1	FormLabs	12.5×12.5×16.5	Y	30×28×45	25	0.4	1.75	300	8	0.004	3.3	Resin	SLA	N
Prox 500	3D Systems	38.1×33×45.7	Y	N/A	80	N/A	N/A	80	N/A	555	500	PLA, Ceramic	SLS	Y
Replicator Z18	Makerbot	30.5×30.5×45.7	Y	49.3×56.5×85.4	N/A	0.4	1.75	100	41	N/A	6.5	ABS,PLA	FDM	Y
3DTouch	3D Systems	27.5×27.5×21	Y	51.5×51.5×59.8	100	N/A	N/A	125	36	15	4.2	PLA,ABS	FDM	Y
Buccaneer	Pirate3D	14.5×12.5×15.5	Y	25.8×25.8×44	N/A	0.4	1.75	85	8	N/A	0.597	PLA	FDM	N
Fortus 900mc	Stratasys	91.4×60.9×91.4	Y	277×168×202	150	N/A	N/A	178	3,287	N/A	400	ABS,PLA	FDM	Y
Object 1000	Stratasys	100×80×50	Y	280×180×180	16	N/A	N/A	85	1,950	N/A	600	120 materials	Polyjet	Y
ORD Bot Hadron	Automation	21.6×21.6×20	Optional	46×49×40	N/A	0.35	1.75	200	N/A	400	0.729	Varies	FDM	N
Creatr	Leapfrog	23×27×20	Y	50×60×50	50	0.35	1.75	150	32	60	1.500	ABS,PLA PVA, Laybrick, Nylon	FDM	Y
Prusa Mendel	Reprap	21.6×21.6×17.8	N	44×47×37	10	0.4	1.75	150	8	N/A	0.799	Varies	FDM	Y
Cube	Cubify	14×14×14	Y	26×26×34	70	N/A	N/A	250	4.3	N/A	1.299	ABS,PLA	PJP	N
Up Plus2	PP3DP	14×14×13.5	Y	24.5×26×35	150	N/A	1.75	150	5	90	1.649	ABS,PLA ABSm	FDM	N

Table V. Materials Supported by 3D Printing Services

	Minimum Wall Thickness (mm)	Minimum Detail (mm)	Accuracy (mm)	Clearance (mm)	Multiple Colors
Polyamide	0.8	0.3	0.3	0.5	Y
Ceramics	3	2	3	4	Y
Silver	0.5	0.3	0.1	N/A	Y
Bronze	0.5	0.3	0.1	N/A	Y
Brass	0.5	0.3	0.1	N/A	Y
Titanium	0.4	0.25	0.2	N/A	Y
High-detail resin	1	0.2	0.1	0.3	N
Alumide	1	0.4	0.3	0.5	Y
ABS	1	0.3	0.2	N/A	Y
Stainless steel	3	0.8	0.25	0.8	Y
Gold	0.5	0.3	0.1	N/A	Y
Upholstery leather	1	N/A	N/A	N/A	Y
Natural wood	3.2	N/A	1	N/A	Y

service companies, Ponoko [2015] features some special materials, such as leather, paper, wood, rubber; i.materialise [2015] provides titanium and polyamide; and Sculpteo [2015] supplies wax. Moreover, these companies all have online model uploading capabilities, shops for selling models, multicolor printing services, and developer application programming interfaces for researchers.

Close attention should be paid when using 3D printing services [Slavkovsky 2012]: printing companies may reject your part several days after you place an order; units, such as millimeters, should be chosen when importing the design; different materials have varying tolerances; and hollowing or redesigning the object to be smaller could save money and time.

5.3. Advantages and Disadvantages of 3D Printing Process

Compared with traditional Subtractive Manufacturing, AM processes are associated with several advantages but also have some limitations because of AM's specialized technology.

5.3.1. Advantages. Because of its additive process, AM offers several advantages over traditional manufacturing methods: increased geometry complexity, convenient digital design and manufacturing, low initial setup costs, global standardized distribution, and environmentally friendly processes [Segerman 2012; Campbell et al. 2011]:

—*Increased Geometry Complexity*: AM offers large amounts of freedom in geometry design because it builds products layer by layer instead of by subtracting from a large piece of material (e.g., cutting and drilling). As a result, it can also produce objects with complex internal structures easily.
—*Convenient Digital Design and Manufacturing*: AM can produce physical parts directly from standardized 3D digital files, which can be created and modified with an easy 3D computer-aided design process. Thus, the time to produce products, especially the design iteration time, can be decreased, and a demo model can be created and tested before mass production to improve companies' economic performances.
—*Low Initial Setup Costs*: AM is a "single-tool" process, which does not need to change the process to match the new product, and it is thus well suited to create customized complex geometries economically.
—*Global Standardized Distribution*: The global distribution of certain products can be rapidly realized due to the standardized 3D digital file formats. The digital file, which

contains the standard design parameters (e.g., print size, resolution, and materials), can be distributed and printed worldwide.

—*Environmentally Friendly Process*: AM is a relatively "green" process because only the material required for the part is efficiently added layer by layer, while traditional Subtractive Manufacturing carves or cuts out the desired parts and leaves behind large amounts of wasted material.

5.3.2. Disadvantages. Although AM technologies offer many benefits, this manufacturing process is still associated with limitations, such as slow printing speed, limited printable area, low uniformity in production quality, unproven durability, and intellectual property and safety concerns:

—*Slow Printing Speed*: AM processes usually create a 1.5-inch cube in approximately 1 hour on average, while a traditional injection-molding machine is capable of making several similar parts in 1 minute. Though the 3D printing speed is increasing, currently, it is still not suitable for mass-production purposes.

—*Limited Printable Area*: Most commonly used 3D printers have a small printable area of approximately 20 cm $\times$ 20 cm $\times$ 20 cm (e.g., Makerbot Replicator 2X), though a few expensive ones can accommodate larger printable areas (e.g., that of the Fortus 900mc is 91.4 cm $\times$ 60.9 cm $\times$ 91.4 cm).

—*Low Uniformity in Production Quality*: Part strength from 3D printing is usually not uniform due to the layer-by-layer fabrication process and the difference in material characteristics. Thus, parts made using different 3D printing machines often have inconsistent properties, although this may also occur in traditional manufacturing.

—*Unproven Durability*: The durability of the machine has not yet been proven in long-term real-world testing. However, it is hoped that a large portion of the machine parts can be printed to replace parts when they are worn out. Currently, the tolerances for the machines are acceptable for many consumer-grade products and Open-Source Appropriate Technology-related components [Pearce et al. 2010].

—*Intellectual Property and Safety Concerns*: As 3D printers become increasingly available to individuals, copyright concerns have been raised, and Greenbaum [2013] proposed an Open Hardware License for 3D printing. Moreover, regarding safety issues, we cannot deny the possibility that people who have 3D printers may print a functional gun based on 3D gun models and use it to commit a crime.

6. A CASE STUDY

3D sensing and printing technologies have dramatically influenced the industrial, medical, cultural, and food production fields and are still reshaping them [Gomes et al. 2014; Willis et al. 2012; Lipson and Kurman 2013]. In this section, we discuss a specific project regarding 3D sensing to printing human head models with realistic hairstyles, conducted by Disney Research and University of Zaragoza, to illustrate the tradeoffs involved in the process of sensing 3D data, postprocessing the 3D model, and finally printing the 3D physical reproduction [Echevarria et al. 2014].

6.1. Case Introduction

One common problem with most 3D human head sensing-to-printing systems is the lack of reproducing hairstyles with detailed stylization and colors. For example, the 3D sensed and printed human head by Figueroa et al. [2013] used only the coarse shape to represent the specific hairstyle. To solve this problem, Echevarria et al. [2014] proposed a method using a multiview algorithm to generate hair as a closed-manifold surface, which contains the structural and color information of the hairstyle. Two examples of their results are shown in Figure 6. To follow is their proposed method:

(A.1) Target stylized hair (A.2) Geometry result (A.3) Final reconstruction result (B.1) Target stylized hair (B.2) Geometry result (B.3) Final reconstruction result

Fig. 6. Stylized hair capture results of two human subjects (A and B) by Echevarria et al. [2014].

First, a smooth surface representation of the scanned hairstyle is generated from a multiview stereo system, which is built by placing 10 digital single-lens reflex cameras in a quarter-spherical setup with four consecutive orientations by 90-degree rotations. Based on a multiview stereo reconstruction algorithm published by Beeler et al. [2010], partial reconstructions from each orientation can be aligned rigidly with the ICP algorithm [Besl and McKay 1992], and then, a single surface, representing the geometric proxy of both hair and face, can be obtained using Poisson reconstruction of the obtained point cloud [Kazhdan et al. 2006].

Second, color information can be divided into low- and high-frequency bands using a Difference of Gaussians filter. Low-frequency information is used to remove visible color seams and attenuate view-dependent color changes, and high-frequency details are sampled only from the single-best view. Because real hair's level of detail is fairly high, a 3D color stylization filter is proposed to reduce the hair complexity while preserving its defining features by extending the 2D color stylization filter to 3D space.

Finally, the per-vertex stylized color is utilized to displace the coherent geometric parts over the surface, stylize the shape, and 3D print the physical reproduction of the reconstructed realistic 3D model, which contains both the geometric and color information of the hairstyle.

6.2. Discussions

Several tradeoffs, such as human intervention, hair complexity simplification, and 3D model miniaturization, have been made during the 3D sensing-to-printing process to improve accuracy, reduce complexity, and increase processing speed:

—*Human Intervention*: To obtain optimal research results, the hair region in the first step is identified manually by researchers. An automatic processing pipeline would reduce human effort and increase the commercialization potential of this technology, though it may decrease the accuracy of the hairstyle reconstruction. Currently, most postprocessing software packages require related knowledge and human intervention for 3D printing preparation, and automatic processing could represent a potential improvement.

—*Hair Complexity Simplification*: The mesh processing time with 300K and 600K hair vertices is fairly long (4 to 7 hours) for this project, even though these numbers of vertices have already been used to generate a result. Reducing the vertices could degrade the color sharpness and geometry details but increase the processing speed. Further optimizing the data structure or utilizing more powerful hardware, such as a GPU, would be good ways to solve this problem.

—*3D Model Miniaturization*: Miniaturizing the 3D models can also reduce the model complexity, improve the processing speed, shorten the 3D printing time, and reduce the 3D print expenses.

Furthermore, shape and matching errors persist in this project, as can be seen in the reconstruction results of a wide range of hairstyles shown in Echevarria et al. [2014]. However, the overall performance of their 3D sensing-to-printing system is still compelling, especially for vivid hair stylization and colors.

7. CONCLUSION

The rapid development of 3D technologies has made them widely available to the public. In this article, we present a comprehensive overview of techniques related to the pipeline from 3D sensing to printing, including 3D scanning and printing devices, as well as techniques from both commercial deployments and published research. A case study is also provided to help readers better understand this 3D reproduction process.

Many commercialized and newly developed 3D technologies are reshaping traditional fields, such as industrial, medical, and cultural areas, and 3D printing is even considered to be the next industrial revolution by many researchers. However, further improvements of these technologies are still needed. For example, 3D sensors and sensing technologies have limitations regarding their sensing environments, sensing duration, target properties, target movements, and many other conditions. Additionally, postprocessing software packages usually require human intervention and related knowledge to implement proper postprocessing steps. Finally, 3D printing technology still suffers from limited printable areas, long printing time, high cost, inability to produce transplantable bio-printed live organs with complete functions, and many other problems.

Although 3D sensing and printing technologies bring substantial benefits to our world, we cannot ignore their potential negative consequences. Easily copying and reproducing objects makes copyright protection more difficult, relying too much on plastics could cause environmental problems, being able to print functional guns or other weapons with CAD-designed models can cause serious safety concerns, and bioprinting may result in moral or ethical issues. All these possible consequences should be kept in mind when developing 3D technologies.

REFERENCES

Mai Adm and Abas Said. 2012. Interactive image-based 3D modeling. In *Proceedings of International Conference on Computer & Information Science*. 1000–1005.

SungHoon Ahn, Michael Montero, Dan Odell, Shad Roundy, and Paul Wright. 2002. Anisotropic material properties of fused deposition modeling ABS. *Rapid Prototyping Journal* 8 (2002), 248–257.

Brett Allen, Brian Curless, and Zoran Popović. 2003. The space of human body shapes: Reconstruction and parameterization from range scans. *ACM Transactions on Graphics* 22 (2003), 587–594.

Dean Anderson, Herman Herman, and Alonzo Kelly. 2005. Experimental characterization of commercial flash ladar devices. In *Proceedings of International Conference of Sensing and Technology*. 17–23.

Luigi Barazzetti, Marco Scaioni, and Fabio Remondino. 2010. Orientation and 3D modelling from markerless terrestrial images: Combining accuracy with automation. *Photogrammetric Record* 25 (2010), 356–381.

Mark Beard, Oana Ghita, and Ken Evans. 2011. Using Raman spectroscopy to monitor surface finish and roughness of components manufactured by selective laser sintering. *Journal of Raman Spectroscopy* 42 (2011), 744–748.

Thabo Beeler, Bernd Bickel, Paul Beardsley, Bob Sumner, and Markus Gross. 2010. High-quality single-shot capture of facial geometry. *ACM Transactions on Graphics* 29 (2010), 40:1–40:9.

Paul Besl and Neil McKay. 1992. A method for registration of 3-D shapes. *IEEE Transactions on Pattern Analysis and Machine Intelligence* 14 (1992), 239–256.

François Blais. 2004. Review of 20 years of range sensor development. *Journal of Electronic Imaging* 13 (2004), 231–243.

Don Brutzman and Leonard Daly. 2010. *X3D: Extensible 3D Graphics for Web Authors*. Morgan Kaufmann.

Thomas Campbell, Christopher Williams, Olga Ivanova, and Banning Garrett. 2011. Could 3D printing change the world? In *Proceedings of Technologies, Potential, and Implications of Additive Manufacturing*. 1–14.

Avishek Chatterjee, Suraj Jain, and Venu Madhav Govindu. 2012. A pipeline for building 3D models using depth cameras. In *Proceedings of the 8th Indian Conference on Computer Vision, Graphics and Image Processing*. 38:1–38.8.

Desai Chen, David Levin, Piotr Didyk, Pitchaya Sitthi-Amorn, and Wojciech Matusik. 2013. Spec2Fab: A reducer-tuner model for translating specifications to 3D prints. *ACM Transactions on Graphics* 32 (2013), 135:1–135:10.

Yang Chen and Gérard Medioni. 1992. Object modelling by registration of multiple range images. *Image and Vision Computing* 10 (1992), 145–155.

Edward Ciaccio, Christina Tennyson, Govind Bhagat, Suzanne Lewis, and Peter Green. 2013. Use of shape-from-shading to estimate three-dimensional architecture in the small intestinal lumen of celiac and control patients. *Computer Methods and Programs in Biomedicine* 111 (2013), 676–684.

Laura Clemente, Andrew Davison, Ian Reid, José Neira, and Juan Tardós. 2007. Mapping large loops with a single hand-held camera. In *Proceedings of the Robotics: Science and Systems Conference*.

Creatform. 2015. Creatform MetraSCAN 210. (2015). Retrieved February 26, 2015, from http://www.creaform3d.com/en.

Yan Cui, Sebastian Schuon, Derek Chan, Sebastian Thrun, and Christian Theobalt. 2010. 3D shape scanning with a time-of-flight camera. In *Proceedings of IEEE Conference on Computer Vision and Pattern Recognition*. 1173–1180.

Yan Cui, Sebastian Schuon, Sebastian Thrun, Didier Stricker, and Christian Theobalt. 2013. Algorithms for 3D shape scanning with a depth camera. *IEEE Transactions on Pattern Analysis and Machine Intelligence* 35 (2013), 1039–1050.

Cyberware. 2015. Cyberware whole body color 3D scanner bundle. (2015). Retrieved February 26, 2015, from http://cyberware.com/pricing/domest-icPriceList.html.

Leonardo De Chiffre, Simone Carmignato, Jean-Pierre Kruth, Robert Schmitt, and Albert Weckenmann. 2014. Industrial applications of computed tomography. *Manufacturing Technology* 63 (2014), 655–677.

Ryan Dehoff, Chad Duty, William Peter, Yukinori Yamamoto, Wei Chen, Craig Blue, and Cory Tallman. 2013. Case study: Additive manufacturing of aerospace brackets. *Advanced Materials & Processes* 171 (2013), 19–22.

Jose Echevarria, Derek Bradley, Diego Gutierrez, and Thabo Beeler. 2014. Capturing and stylizing hair for 3D fabrication. *ACM Transactions on Graphics* 33 (2014), 125:1–125:11.

Stephen Ellerin. 2004. The art and science of 3D printing. *Emedia* 17 (2004), 14.

EosSystems. 2015. Photomodeler. (2015). Retrieved February 26, 2015, from http://www.photomodeler.com/index.html.

Jacques Feldmar and Nicholas Ayache. 1996. Rigid, affine and locally affine registration of free-form surfaces. *International Journal of Computer Vision* 18 (1996), 99–119.

Nadia Figueroa, Haiwei Dong, and Abdulmotaleb El Saddik. 2013. From sense to print: Towards automatic 3D printing from 3D sensing devices. In *Proceedings of IEEE International Conference on Systems, Man, and Cybernetics*. 4897–4904.

Timothy Fish. 2011. *Extending Art of Illusion: A Reference for Creating Plugins and Scripts*. Timothy Fish.

Yasutaka Furukawa and Jean Ponce. 2010. Accurate, dense, and robust multiview stereopsis. *IEEE Transactions on Pattern Analysis and Machine Intelligence* 32 (2010), 1362–1376.

Gartner. 2015. Cool Vendors in 3D Printing. (2015). Retrieved February 26, 2015, from https://www.gartner.com/doc/2471215/cool-vendors-d-printing.

Burak Gokturk, Hakan Yalcin, and Cyrus Bamji. 2004. A time-of-flight depth sensor-system description, issues and solutions. In *Proceedings of Computer Vision and Pattern Recognition Workshop*. 35–35.

Leonardo Gomes, Olga Bellon, and Luciano Silva. 2014. 3D reconstruction methods for digital preservation of cultural heritage: A survey. *Pattern Recognition Letters* 50 (2014), 3–14.

Eli Greenbaum. 2013. Three-dimensional printing and open source hardware. *Journal of Intellectual Property and Entertainment Law at New York University* 2 (2013), 257–369.

Alper Hacıoğlu. 2014. *GNU-General Public License*.

Miles Hansard, Seungkyu Lee, Ouk Choi, and Radu Patrice Horaud. 2012. *Time-of-Flight Cameras: Principles, Methods and Applications*. Springer Science & Business Media.

Peter Henry, Michael Krainin, Evan Herbst, Xiaofeng Ren, and Dieter Fox. 2014. RGB-D mapping: Using depth cameras for dense 3D modeling of indoor environments. In *Proceedings of Experimental Robotics*. 477–491.

Joan Horvath. 2014. A brief history of 3D printing. In *Mastering 3D Printing*. Springer, Berlin, 3–10.

Cătălin Iancu, Daniela Iancu, and Alin Stăncioiu. 2010. From CAD model to 3D print via “STL” file format. *Fiability & Durability* 1 (2010), 73–80.

Katsushi Ikeuchi. 2001. Modeling from reality. In *Proceedings of the 3rd IEEE International Conference on 3-D Digital Imaging and Modeling*. 117–124.

i.materialise. 2015. i.materialise. (2015). Retrieved February 26, 2015, from http://i.materialise.com/.

Shahram Izadi, David Kim, Otmar Hilliges, David Molyneaux, Richard Newcombe, Pushmeet Kohli, Jamie Shotton, Steve Hodges, Dustin Freeman, Andrew Davison, and Andrew Fitzgibbon. 2011. KinectFusion: Real-time 3D reconstruction and interaction using a moving depth camera. In *Proceedings of the 24th Annual ACM Symposium on User Interface Software and Technology*. 559–568.

Bahram Javidi, Myungjin Cho, Inkyu Moon, Arun Anand, Manuel Martinez-Corral, Adrian Stern, Abhijit Mahalanobis, and Zeev Zalevsky. 2013. 3D imaging and visualization: An overview of recent advances. In *Proceedings of Workshop on Information Optics*. 1–3.

Yunsuk Kang and Yosung Ho. 2010. High-quality multi-view depth generation using multiple color and depth cameras. In *Proceedings of IEEE International Conference on Multimedia and Expo*. 1405–1410.

Hadi Kaveh, Mohammad-Shahram Moin, and Farbod Razzazi. 2013. A novel steganography approach for 3D polygonal meshes using surfacelet transform. In *Proceedings of the 8th Iranian Conference on Machine Vision and Image Processing*. 304–309.

Michael Kazhdan, Matthew Bolitho, and Hugues Hoppe. 2006. Poisson surface reconstruction. In *Proceedings of the 4th Eurographics Symposium on Geometry Processing*.

Richard Ketcham and William Carlson. 2001. Acquisition, optimization and interpretation of X-ray computed tomographic imagery: Applications to the geosciences. *Computers & Geosciences* 27 (2001), 381–400.

Kourosh Khoshelham and Sander Oude Elberink. 2012. Accuracy and resolution of kinect depth data for indoor mapping applications. *Sensors* 12 (2012), 1437–1454.

Kinect. 2010. Kinect v1. (2010). Retrieved February 26, 2015, from http://www.microsoft.com/en-us/kinectforwindows/.

Ahmed Kirmani, Arrigo Benedetti, and Philip A. Chou. 2013. Spumic: Simultaneous phase unwrapping and multipath interference cancellation in time-of-flight cameras using spectral methods. In *Proceedings of IEEE International Conference on Multimedia and Expo*. 1–6.

Andreas Kolb, Erhardt Barth, Reinhard Koch, and Rasmus Larsen. 2009. Time-of-flight sensors in computer graphics. In *Proceedings of Eurographics (State-of-the-Art Report)*. 119–134.

Jean Pierre Kruth, Markus Bartscher, Simone Carmignato, Robert Schmitt, Leonardo De Chiffre, and Albert Weckenmann. 2011. Computed tomography for dimensional metrology. *Manufacturing Technology* 60 (2011), 821–842.

Robert Lange and Peter Seitz. 2001. Solid-state time-of-flight range camera. *IEEE Journal of Quantum Electronics* 37 (2001), 390–397.

Marc Levoy, Kari Pulli, Brian Curless, Szymon Rusinkiewicz, David Koller, Lucas Pereira, Matt Ginzton, Sean Anderson, James Davis, Jeremy Ginsberg, et al. 2000. The digital Michelangelo project: 3D scanning of large statues. In *Proceedings of the 27th Annual Conference on Computer Graphics and Interactive Techniques*. 131–144.

Hod Lipson and Melba Kurman. 2013. *Fabricated: The New World of 3D Printing*. John Wiley & Sons.

Hod Lipson, Francis C. Moon, Jimmy Hai, and Carlo Paventi. 2005. 3-D printing the history of mechanisms. *Journal of Mechanical Design* 127 (2005), 1029–1033.

Kai Liu, Yongchang Wang, Daniel Lau, Qi Hao, and Laurence Hassebrook. 2010a. Dual-frequency pattern scheme for high-speed 3-D shape measurement. *Optics Express* 18 (2010), 5229–5244.

Kai Liu, Yongchang Wang, Daniel Lau, Qi Hao, and Laurence Hassebrook. 2010b. Gamma model and its analysis for phase measuring profilometry. *Journal of the Optical Society of America A* 27 (2010), 553–562.

Shoubin Liu and Wenguang Niu. 2012. A novel algorithm for segmentation of complex point cloud with 3D elastic model. In *Proceedings of International Conference on Computer Science and Automation Engineering*. 407–411.

Diego Manfredi, Flaviana Calignano, Manickavasagam Krishnan, Riccardo Canali, Elisa Paola Ambrosio, and Eleonora Atzeni. 2013. From powders to dense metal parts: Characterization of a commercial AlSiMg alloy processed through direct metal laser sintering. *Materials* 6 (2013), 856–869.

Julie Marcoux and Kenneth-Roy Bonin. 2012. Three dimensional printing: An introduction for information professionals. In *Proceedings of the 6th International Conference on Digital Society*. 54–58.

Primoz Markelj, Dejan Tomaževič, Bostjan Likar, and Franjo Pernuš. 2012. A review of 3D/2D registration methods for image-guided interventions. *Medical Image Analysis* 16 (2012), 642–661.

MenciSoftware. 2015. Menci. (2015). Retrieved February 26, 2015, from http://www.menci.com/.

MESA-Imaging. 2015. SwissRanger 4500. (2015). Retrieved February 26, 2015, from http://www.mesa-imaging.ch/swissranger4500.php.

Microsoft. 2015. Microsoft Kinect. (2015). Retrieved February 26, 2015, from http://www.microsoft.com/en-us/kinectforwindows/.

Simone Milani and Giancarlo Calvagno. 2011. A cognitive approach for effective coding and transmission of 3D video. *ACM Transactions on Multimedia Computing, Communications, and Applications* 7S (2011), 23:1–23:21.

Tobias Möller, Holger Kraft, Jochen Frey, Martin Albrecht, and Robert Lange. 2005. Robust 3D measurement with Pmd sensors. In *Proceedings of the 1st Range Imaging Research Day*. 8.

Kamran Mumtaz and Neil Hopkinson. 2010. Selective laser melting of thin wall parts using pulse shaping. *Journal of Materials Processing Technology* 210 (2010), 279–287.

Richard A. Newcombe, Andrew J. Davison, Shahram Izadi, Pushmeet Kohli, Otmar Hilliges, Jamie Shotton, David Molyneaux, Steve Hodges, David Kim, and Andrew Fitzgibbon. 2011. KinectFusion: Real-time dense surface mapping and tracking. In *Proceedings of IEEE International Symposium on Mixed and Augmented Reality*. 127–136.

North-Star-Imaging. 2015. X-View X5000. (2015). Retrieved February 26, 2015, from http://www.xviewct.com/industrial-ct-systems/x-view-computed-tomography/m5000-series.

Rachel Opitz, Katie Simon, Adam Barnes, Kevin Fisher, and Lauren Lippiello. 2012. Close-range photogrammetry vs. 3D scanning: Comparing data capture, processing and model generation in the field and the lab. In *Proceedings of Computer Applications and Quantitative Methods in Archaeology Conference*.

Tong Pan, Xiao Jing Li, Hao Peng Wang, and Ting Ting Liu. 2013. Research on method of 3D models viewpoint control based on VRML. *Advanced Materials Research* 753 (2013), 1283–1286.

Narendra Patel and Mukesh Zaveri. 2012. 3D model reconstruction and animation from single view face image. In *Proceedings of International Conference on Audio, Language and Image Processing*. 674–682.

Joshua Pearce, Morris Blair, KI Laciak, Rob Andrews, Amir Nosrat, and Ivana ZelenikaZovko. 2010. 3-D printing of open source appropriate technologies for self-directed sustainable development. *Journal of Sustainable Development* 3 (2010), 17–29.

Jeanne Pellerin, Bruno Lévy, Guillaume Caumon, and Arnaud Botella. 2014. Automatic surface remeshing of 3D structural models at specified resolution: A method based on Voronoi diagrams. *Computers & Geosciences* 62 (2014), 103–116.

Bre Pettis, Anna Kaziunas France, and Jay Shergill. 2012. *Getting Started with MakerBot*. O'Reilly Media.

Ponoko. 2015. Ponoko. (2015). Retrieved February 26, 2015, from https://www.ponoko.com/.

JiannYeou Rau and PoChia Yeh. 2012. A semi-automatic image-based close range 3D modeling pipeline using a multi-camera configuration. *Sensors* 12 (2012), 11271–11293.

Fabio Remondino and Sabry El-Hakim. 2006. Image-based 3D modelling: A review. *Photogrammetric Record* 21 (2006), 269–291.

Martijn Rooker, Alfred Angerer, Jose Capco, Christoph Heindl, Aitor Olarra, Elena Fuentes, Christian Wögerer, and Andreas Pichler. 2013. Flexible grasping of electronic consumer goods. In *Robotics in Smart Manufacturing*. Springer, Berlin, 158–169.

Joaquim Salvi, Sergio Fernandez, Tomislav Pribanic, and Xavier Llado. 2010. A state of the art in structured light patterns for surface profilometry. *Pattern Recognition* 43 (2010), 2666–2680.

Giovanna Sansoni, Marco Trebeschi, and Franco Docchio. 2009. State-of-the-art and applications of 3D imaging sensors in industry, cultural heritage, medicine, and criminal investigation. *Sensors* 9 (2009), 568–601.

Sculpteo. 2015. Sculpteo. (2015). Retrieved February 26, 2015, from http://www.sculpteo.com/en/.

Henry Segerman. 2012. 3D printing for mathematical visualisation. *Mathematical Intelligencer* 34 (2012), 1–7.

Ed Sells, Zach Smith, Sebastien Bailard, Adrian Bowyer, and Vik Olliver. 2009. RepRap: The Replicating Rapid Prototyper - maximizing customizability by breeding the means of production. In *Handbook of Research in Mass Customization and Personalization*, F. T. Piller and M. M. Tseng (Eds.). Vol. 1. World Scientific, 568–580.

Shapesways. 2015. Shapesways. (2015). Retrieved February 26, 2015, from http://www.shapeways.com/.

Jamie Shotton, Andrew Fitzgibbon, Mat Cook, Toby Sharp, Mark Finocchio, Richard Moore, Alex Kipman, and Andrew Blake. 2011. Real-time human pose recognition in parts from single depth images. In *Proceedings of IEEE Conference on Computer Vision and Pattern Recognition*. 129–134.

Elizabeth Ann Slavkovsky. 2012. *Feasibility Study for Teaching Geometry and Other Topics Using Three-Dimensional Printers*. Master's thesis. Harvard University.

Jan Smisek, Michal Jancosek, and Tomas Pajdla. 2013. 3D with Kinect. In *Consumer Depth Cameras for Computer Vision*. Springer, London, 3–25.

Elena Stoykova, A. Aydin Alatan, Philip Benzie, Nikolaos Grammalidis, Sotiris Malassiotis, Joern Ostermann, Sergej Piekh, Ventseslav Sainov, Christian Theobalt, Thangavel Thevar, et al. 2007. *IEEE Transactions on Circuits and Systems* 17 (2007), 1568–1586.

Jürgen Sturm, Erik Bylow, Fredrik Kahl, and Daniel Cremers. 2013. CopyMe3D: Scanning and printing persons in 3D. In *Pattern Recognition*. Springer, Berlin, 405–414.

3D Systems. 2015. 3D Systems. (2015). Retrieved February 26, 2015, from www.3dsystems.com.

Liangwen Tang, Sheng Yang, Nong Cheng, and Qing Li. 2014. Toward autonomous navigation using an RGB-D camera for flight in unknown indoor environments. In *Proceedings of IEEE Chinese Guidance, Navigation and Control Conference*. 2007–2012.

LMI Technologies. 2015. HDI Advance R3x. (2015). Retrieved February 26, 2015, from http://www.creaform3d.com/en.

Jing Tong, Jin Zhou, Ligang Liu, Zhigeng Pan, and Hao Yan. 2012. Scanning 3D full human bodies using kinects. *IEEE Transactions on Visualization and Computer Graphics* 18 (2012), 643–650.

Toshiba. 2015. TOSCANER 20000AV. (2015). Retrieved February 26, 2015, from http://www.toshiba-itc.com/cat/en/prod01.html.

Ben Utela, Duane Storti, Rhonda Anderson, and Mark Ganter. 2008. A review of process development steps for new material systems in three dimensional printing (3DP). *Journal of Manufacturing Processes* 10 (2008), 96–104.

Boštjan Vaupotič, Miran Brezočnik, and Jože Balič. 2006. Use of PolyJet technology in manufacture of new product. *Journal of Achievements in Materials and Manufacturing Engineering* 18 (2006), 1–2.

Kiril Vidimče, Szu-Po Wang, Jonathan Ragan-Kelley, and Wojciech Matusik. 2013. OpenFab: A programmable pipeline for multi-material fabrication. *ACM Transactions on Graphics* 32 (2013), 136.

Jinfeng Wang and Guoqing Yao. 2011. Obj three-dimensional model file format in OpenGL, input and processing. *Computer Knowledge and Technology* 10 (2011), 068.

Jianfeng Wang, Cha Zhang, Wenwu Zhu, Zhengyou Zhang, Zixiang Xiong, and Philip A. Chou. 2012. 3D scene reconstruction by multiple structured-light based commodity depth cameras. In *Proceedings of IEEE International Conference on Acoustics, Speech and Signal Processing*. 5429–5432.

Udaya Wijenayake, SeungHae Baek, and SoonYong Park. 2012. An error correcting 3D scanning technique using dual pseudorandom arrays. In *Proceedings of International Conference on 3D Imaging, Modeling, Processing, Visualization and Transmission*. 517–523.

Karl Willis, Eric Brockmeyer, Scott Hudson, and Ivan Poupyrev. 2012. Printed optics: 3D printing of embedded optical elements for interactive devices. In *Proceedings of the 25th Annual ACM Symposium on User Interface Software and Technology*. 589–598.

Genyuan Xia and Li Chen. 2014. 3D dental mesh repairing using template-based deformation. In *Proceedings of the 7th International Conference on Biomedical Engineering and Informatics*. 410–414.

Lin Yang, Longyu Zhang, Haiwei Dong, Abdulhameed Alelaiwi, and Abdulmotaleb El Saddik. 2015. Evaluating and improving the depth accuracy of Kinect for Windows v2. *IEEE Sensors Journal* 15 (2015), 4275–4285.

Klemen Žbontar, Matjaž Mihelj, Boštjan Podobnik, Franc Povše, and Marko Munih. 2013. Dynamic symmetrical pattern projection based laser triangulation sensor for precise surface position measurement of various material types. *Applied Optics* 52 (2013), 2750–2760.

Longyu Zhang, Jamal Saboune, and Abdulmotaleb El Saddik. 2014. Transforming a regular screen into a touch screen using a single webcam. *Journal of Display Technology* 10 (2014), 647–659.

Zhengyou Zhang. 1994. Iterative point matching for registration of free-form curves and surfaces. *International Journal of Computer Vision* 13 (1994), 119–152.

Zheng Zhang and Hock Soon Seah. 2012. CUDA acceleration of 3D dynamic scene reconstruction and 3D motion estimation for motion capture. In *Proceedings of International Conference on Parallel and Distributed Systems*. 284–291.

Yin Zhou, Kai Liu, Jinglun Gao, Kenneth Barner, and Fouad Kiamilev. 2013. High-speed structured light scanning system and 3D gestural point cloud recognition. In *Proceedings of IEEE Conference on Information Sciences and Systems*. 1–6.

Jiejie Zhu, Liang Wang, Ruigang Yang, and James Davis. 2008. Fusion of time-of-flight depth and stereo for high accuracy depth maps. In *Proceedings of IEEE Conference on Computer Vision and Pattern Recognition*. 1–8.

Shiping Zhu and Jie Gao. 2012. 3D modeling and rendering based on uncalibrated single view image in undergraduate final design. In *Proceedings of International Conference on Computer Science and Information Processing*. 1336–1340.

Received September 2014; revised July 2015; accepted July 2015